Journal of Heat and Mass Transfer Research

Journal homepage: https://jhmtr.semnan.ac.ir

Semnan University

ISSN: 2383-3068

Research Article

Thermo-Economic Evaluation of the Combined Power, Heat and Cooling Production System Integrating Gas Turbine and Absorption Cooling

Ali Eyvazi, Mohammad Shafiey Dehaj *

Department of Mechanical Engineering, Vali-e-Asr University of Rafsanjan, Rafsanjan, Iran

ARTICLE INFO

Article history:

Received: 2024-03-17

Revised: 2024-05-18

Accepted: 2024-06-24

Keywords:

Absorption cooling;

Co-Production;

Economic evaluation;

Exergy evaluation;

Gas turbine.

ABSTRACT

In this research, a combined cooling system of heating and electricity is proposed and a complete thermodynamic analysis is presented. The system includes a gas turbine, a heat cooling system, a cogeneration system and a hot water heat exchanger. The basis of the work is that by using the recovery of waste gases in the gas turbine can be generated by a steam turbine and, with the help of an absorption chiller, can recover the waste heat in the steam turbine and provide the required cooling. The cogeneration system saves energy consumption, and reduces environmental pollution. In this study, we have tried to increase the economic justification of using the cogeneration system under study by using up-to-date cost functions. The energy efficiency and exergy efficiency of the studied system are 20 and 21%, respectively, which is a reasonable amount. The results of the economic analysis show that with a total cost of $ 93.56 per second and a total investment and maintenance cost of $ 1732 per second, the proposed system is highly economical and profitable in practice. This may provide a new way to increase the efficiency and effectiveness of thermodynamic performance of cogeneration systems.

1. Introduction

Today, due to the growing need of human society to generate electricity and electricity, the use of natural resources and fossil fuels to achieve this has increased. Exhaustion of fossil fuels along with pollution of these fuels has attracted the attention of energy policymakers and political rulers in different countries of the world on the use of renewable resources and improving the efficiency and effectiveness of equipment and facilities based on fossil fuels [1]. Extensive utilization of clean energy, significant reduction of pollutant emissions and pursuit of higher energy conversion efficiency are promising solutions to alleviate the ever-increasing demand for fossil fuel and severe environmental pollution [2], [3]. Enhancement of building energy consumption to reach increased thermal comfort has become a global crisis due to the depletion of fossil fuel resources and related environmental problems [4]. One of the paramount requirements for satisfying global energy standards is the development of alternative energy sources. As an example, today, manufacturing and untiring solar stills, which produce freshwater without polluting the environment, besides, at a low cost, have been considered a suitable solution to eliminate the

* **Corresponding author.**
E-mail address: m.shafiey@vru.ac.ir

Cite this article as:

Eyvazi, A. and Shafiey Dehaj, M., 2025. Thermo-Economic Evaluation of the Combined Power, Heat and Cooling Production System Integrating Gas Turbine and Absorption Cooling. *Journal of Heat and Mass Transfer Research*, 12(1), pp. 29-44.

https://doi.org/10.22075/JHMTR.2024.33565.1536

shortage of fresh water [5]. These types of resources are incorporated in plans to reduce the greenhouse gas emissions caused by fossil fuels [6]. Among the various medium- and high-temperature heat sources, nuclear energy has developed rapidly in recent years due to its advantages in terms of friendliness, economy, and reliability. Especially with the gradual maturity of Gen IV nuclear reactors, nuclear energy has a bright future in the field of power generation [7]. Simultaneous generation of electricity, heat and cold systems is one of the technologies based on fossil fuels that in addition to generating electricity, from the lost heat to meet the heating and cooling needs of domestic and industrial consumers and save energy, increase economic efficiency and reduce environmental pollution. Developing renewable energy and improving energy utilization efficiency are regarded as effective solutions. Recently, distributed energy systems (DESs) with multi-form outputs, investment saving, and low carbon emissions have been recognized as a promising approach. Combined cooling, heating, and power (CCHP) systems are a typical form of a DES and have become an active topic of research because they effectively promote energy utilization efficiency and reduce pollutant emissions. The gas turbine cycle (GTC) has the advantages of quick start-up, strong fuel adaptability, short construction period, and low pollution emissions, and has been widely employed in DESs as the main power generation unit. However, a stand-alone GTC unit without a waste heat recovery system (WHRS) often features relatively low fuel use efficiency and a large amount of heat dissipation. Thus, it is important to integrate the design of the WHRS with the GTC [8]. If we add the production of cold to the simultaneous production of electricity and heat in the cogeneration system, the cogeneration system of power, heat and cold is obtained. The generated cold is obtained by adding an absorption chiller such as a hot water chiller, hot water and water vapor to the cogeneration system. The heat required in the chiller generator is generated in parallel by the cogeneration system according to the type of chiller, which can be a hot water or steam boiler. Heat losses are recovered by the heat recovery system and the cooling needs of the building are met in summer and by transferring part of this heat to the absorption chiller, cold is and another part of the heat lost in winter is used for heating the building. For times when the operation of the cogeneration system stops for any unpredictable and unavoidable reason, an auxiliary boiler eliminates the interruption and the required heat and cold are obtained. Jiang et al. Evaluated a cogeneration system equipped with a dehumidification system and a hybrid refrigeration system. The refrigeration hybrid system includes an absorption and compression system. Their design and optimization are based on a thermal-economic model. Their proposed model was very effective in decision-making to reduce running costs and investment [9]. Zhang et al. conducted a comprehensive study on different absorption power cycles driven by the waste heat of the sCO_2 cycle. The superiority of the sCO_2/APC system was also verified through thermodynamic and thermoeconomic analysis [10]. Fan et al. developed a combined cooling, heating and power (CCHP) system consisting of a sCO2 system, an ejector refrigeration cycle (ERC) and an ORC. The results revealed that the novel CCHP system could increase exergy efficiency by 9.17% and decrease the total product unit cost by 5.05% [11]. Yuan et al. proposed a combined cooling and power (CCP) system in which the CO2 was used as the only working fluid. They compared the performance of the novel CCP system and two separated CCP systems and concluded that the proposed system was suitable for lower turbine inlet pressures compared with separated CCP systems. Besides, the absorption refrigeration cycle (ARC) is also suitable for utilizing low-grade heat to produce cooling capacity [12]. Wu et al. investigated a combined sCO2/ammonia-water ARC system by thermodynamic and thermoeconomic analysis. They reported that the ARC could achieve the purpose of cooling and power generation and improve system performance significantly [13]. Martín-Hernández et al. investigated three methods of amine absorption, pressure swing adsorption, and membrane separation to produce bioCH_4 simultaneously with CO_2 capture and determine the optimal operating condition. The results indicated that applying the pressure swing adsorption method using zeolite 13X with CO_2 capture had the most economical production and investment costs [14]. Mehrpooya et al. performed the exergoeconomic and exergoenvironmental analyses to evaluate a refrigeration production structure using the absorption-compression refrigeration process and ORC. The irreversibility and exergy efficiency of the proposed process were 83.4 kW and 69%, respectively [15]. Ghorbani et al. developed an integrated structure for the cogeneration of liquefied natural gas and liquefied carbon dioxide using biogas treatment units and a mixed fluid cascade process. The results showed that the specific energy consumption, total energy, and exergy efficiencies were 0.4761 kWh/kg bioLNG, 0.7311, and 0.7258, respectively [16]. Hosseini et al. investigated a system of biogas to electricity by solid oxide fuel cell. The two solutions of direct injection of biogas into SOFC, as well as

purification of biogas, have been first compared, and injection of treated biogas into SOFC has been then compared with each other. The results explain that the system operates better in the conditions of using pre-process biogas upgrading so that the energy and exergy efficiencies in these conditions have been achieved by 51.10% and 52.3%, respectively. Energy and exergy efficiencies of 37.2% and 38.6% would be achieved in the direct injection of untreated biogas into SOFC [17]. Ebrahimi et al. developed an innovative integrated structure for the cogeneration of biomethane (bioCH4) and liquid carbon dioxide (CO2) by unrefined biogas and exhaust fumes from power plants. Their economic assessment indicated that the return period and the prime cost of the product are equal to 4.45 years and 0.8189 US$/ m3 bio-methane, respectively. Also, The sensitivity investigation showed that the total thermal efficiency increases up to 72.50% and geothermal heat duty decreases to 7808 kW with the enhancement of methane composition in the untreated biogas from 55 mol% to 75 mol% [18]. Jing et al. Developed an evaluation model that combines fuzzy theory with multifunctional decision-making to evaluate the economics of a cogeneration system and a hybrid weight measurement method to compare the performance of a cogeneration system set up by natural gas, solar cell, and composite system. They studied steam gas [19]. Wang et al. Examined the combined cogeneration system run by the solar system, which is a combination of the Rankin cycle and the ejector refrigerator cycle, and evaluated the effect of the velocity angle and the slope angle of the solar system diagram. Research has led to the conclusion that the optimal slope angle is 45 degrees and the proper velocity angle is 60 degrees, and in these conditions, the exergy efficiency can be increased to 60% [20]. Gu et al. Studied cogeneration systems using three methods of energy consumption called thermal tracking, electrical tracking and island method, and based on the results and documents, concluded that the cogeneration system based on gas engine fuel and fuel cells have high efficiency in terms of energy and environment, but they are not economically feasible [21]. Yan and his colleagues examined the technical and economic aspects of the Beijing cogeneration system, the technology structure, and the economic benefits of cogeneration systems. The results of their work showed that the gas cogeneration system has good profitability for the consumer, and a reasonable ratio of energy efficiency can help to recover investment in the gas cogeneration system [22]. Li et al. Studied a cogeneration system at a hotel in China and concluded that the annual cost increases and then decreases as the system capacity increases and that the price of energy used affects the system capacity and cooling ratio and increases. The price of natural gas reduces the capacity of the system and increases the cooling ratio [23]. Wang et al. Examined the co-production system of a heat storage tank in a restaurant, which received the required power from a micro turbine, and concluded that the use of heat storage increases investment costs and energy consumption and prolongs life. The system shrinks annually and has no economic justification [24]. Okamoto et al. Evaluated and analyzed the energy demand in a hospital and examined the system of simultaneous production of heat and cold power in the hospital. Implementation and operation of the system had no technical obstacles, and their research results showed energy savings, reducing the cost of the hospital in transferring energy to the hospital, meeting the heating and cooling needs and electricity in cases of power outages and reducing carbon dioxide emissions [25]. Bruno et al. proposed a direct fuel adsorption system in which a gas micro turbine was connected directly to a dual-effect adsorption chiller. The results showed that the system performance coefficient was higher than single-effect absorption chillers. In addition, the cogeneration system with a small-scale gas turbine and a two-effect absorption chiller has been widely used. A single-effect absorption refrigeration cycle with a gas turbine is another co-production system technology that allows the cycle to operate at two different temperature levels and improves exhaust gas recycling [26]. Kong et al. Evaluated the energy efficiency, economic feasibility, and exergy of a Stirling-driven cogeneration system. The Sterling engine operates as a source of energy supply based on external combustion, which has a very low cycle speed and heat transfer in the same temperature process, and their research results indicate that they help to conserve fuel sources and provide economic benefits. [27]. Ghaebi et al. Performed energy, exergy and thermoeconomic analysis on the cogeneration system, which includes air compressor, combustion chamber, gas turbine, dual pressure heat recovery steam generator and absorption chiller. The effects of parameters such as air compressor pressure ratio on the thermodynamic performance of this system have been investigated. The results of the exergy evaluation showed that the greatest exergy degradation occurs in the combustion chamber due to the temperature difference for heat transfer between the working flame and the fluid and the irreversible nature of the chemical reactions [28]. Fan et al. Evaluated the thermodynamic performance of the gas engine

cogeneration system under external design conditions. With the aim of developing combined cooling and power systems to generate electricity and cooling, they studied the use of medium temperature heat sources in the form of cascading and achieving better thermal adaptation of heat recovery processes [29]. Tamm et al. By studying the energy and exergy of a system of simultaneous generation of electricity and cooling, which included a water-ammonia Rankine cycle and an absorption refrigeration cycle, realized its high thermal efficiency compared to other systems and using different heat sources such as Solar energy, industrial output heat and geothermal sources had high flexibility and efficiency and showed its high justification [30].

Han et al. Developed a new heat-based refrigeration system with a heat-based compression subsystem and an adsorption refrigeration subsystem and found that the same inlet heat produced 46.7% colder than the conventional water-ammonia absorption refrigeration system. Heat-based hybrid refrigeration systems can use extra heat. In this research, in order to make more use of the high temperature heat of the exhaust gas from the gas turbine and to promote the use of energy cascade, a new cogeneration system is proposed and evaluated. This system includes a gas turbine, a water-ammonia turbine, a single-wall water absorption refrigerator and a hot water exchanger [31]. Chua et al. Have studied the different configurations of the cogeneration system with different types of mobile motion technologies such as micro-turbines, solar sterling vessels and fuel cell systems with the help of panels and biomass of wood chips. These systems are designed for a tourist island in Singapore. Among the various combinations of technologies, the economically optimal case leads to 20% penetration of renewable energy and savings of up to one thousand tons of carbon dioxide per year [32]. Calise et al. Simulated an innovative multiple generation system that generates geothermal energy as well as solar energy to supply electricity, heating, cooling, and drinking water to a volcanic island in the southern Mediterranean. Photovoltaic/ thermal solar collectors can provide a maximum of 800 kWh of electricity with a space heating capacity of 700 kW, a cooling capacity of 900 kW and domestic hot water with a nominal capacity of 3900 kW. The system can also produce 2.71 kg / s of drinking water using heat from solar and geothermal systems. This means saving about 5,000 tons of carbon dioxide emissions per year and producing 418,000 tons per year of fresh water [33]. Another economical-thermal analysis of a small-scale cogeneration system located on a Greek island was presented by Karellas et al. An Organic Organic Cycle (ORC) operated by a biomass boiler and solar heat collectors can provide 1.42 kilowatts of electricity and about 50 kilowatts of thermal power. The estimated repayment period varies between four and 18 years depending on investment costs and biomass prices, but in all cases, it performs better than the reference system [34]. Valipour et al. provided the application of Thermal-Economic Multi-Objective Optimization of Shell and Tube Heat Exchanger Using the Multi-Objective Big Bang-Big Crunch algorithm (MOBBA) technique. They used the MOBBA method to obtain the maximum effectiveness (heat recovery) and the minimum total cost as two objective functions [35].

In this paper, in order to optimally use high temperature waste heat from gas turbine outlet, a new CCHP system is proposed and evaluated. This system consists of a gas turbine, an ammonia-water turbine, a LiBr-H2O absorption refrigerator and a hot water heat exchanger. In addition, thermodynamic performance benefits are demonstrated using a comprehensive comparison with the reference system. An exergy and energy analysis are then completed under the design conditions to reveal the energy saving mechanism. As it is clear, most previous studies have used energy, exergetic or thermoeconomic studies separately to analyze CCHP systems. Energy analysis or the first law may give ideal answers for the operation of a cycle and cannot show irreversibility in the various components of the system. Also, each of the exergetic and thermoeconomic analyzes cannot provide a suitable tool for the analysis of energy systems. Therefore, in this paper, using a combination of energy analysis, exergy and thermoeconomic based on Brayton cycle waste heat recovery and single-effect absorption cooling, which is economical, a more general and detailed analysis of a CCHP system is carried out. Here, the effects of operational parameters on fuel consumption, cold, heat and net power output, first and second law efficiency, exergy destruction in each of the system components and the total operational and capital costs of the system are examined in detail.

2. System Description

The system consists of a gas turbine, a combined cooling and power subsystem and a heat exchanger, as shown in figure 1. At point 1, the air is compressed to a higher pressure and temperature by the compressor. Compressed air enters the combustion chamber at point 2, where the combustion process takes place. At point 3, the combustion mixture enters the turbine to generate electricity. In the water-ammonia Rankine cycle, the water-ammonia base solution

at point 10 is first pumped by pump 1 at point 7 and then flows into a helical tube. A recovered steam generator in which it is converted to point 8 superheated ammonia steam with exhaust heat coming out of the generator. Point 8 superheated ammonia vapor expands in axial flow turbine 2 to generate electrical power. The dense heat of ammonia vapor point 9 and the vapor and liquid heat of point 10 then provide the heat required to produce the lithium bromide water absorption refrigeration subsystem. Points 7, 8, 9, and 10 indicate a change in the ammonia Rankine cycle. The single-acting water-lithium bromide absorption refrigeration cycle consists of a condenser, generator, evaporator, absorber, heat exchanger, pump and two expansion valves. The diluted lithium bromide solution collects on the bottom of the absorber. From this part, a solution pump leads to a tube shell converter to preheat.

After leaving the converter, the dilute solution is directed to the top of the chiller. The dilute lithium bromide solution is surrounded by copper tubes with steam or hot water or hot water flowing through them. Hot water, steam or hot water transfer heat to the dilute solution. The solution boils and the water vapor separates from the solution and enters the condenser located at the top of the generator, where the remaining solution in the generator is concentrated. The concentrated solution is transferred to a heat exchanger to lose its temperature in exchange for the solution being pumped to the generator. The refrigerant vapor produced in the generator is transferred to the condenser by means of copper pipes in which the water of the cooling tower flows, which is so-called condensate and collects in the bottom pan of the condenser. The refrigerant is transferred from the condenser to the evaporator, and according to the model and manufacturer of the chiller, it is usually sprayed on the copper pipes of the evaporator, and according to the vacuum, the water boils at a temperature of 3.9 ° C. This causes the water to boil, and the water of the ventilation system inside the copper pipes cools down by losing temperature and transferring the temperature to the refrigerant, and the refrigerant boils, and water vapor is produced in the evaporator. Since the evaporator and the absorber part are connected to each other, the water vapor produced in the evaporator is transferred to the absorber and a thick lithium spray is transferred from the generator to the heat exchanger and then to the absorber sprays due to its absorbent lithium property. The steam produced in the evaporator absorbs lithium bromide, and the solution is diluted. It should be noted that the absorption of moisture by lithium bromide generates heat, which is dissipated by copper pipes in which the cooling tower water flows, and now the lithium bromide solution is collected at the bottom of the chiller and pumped again. The solution is pumped. The gas turbine cycle consists of four internal reversible processes. In an isentropic compressor, a constant pressure transfer of heat takes place in a heat exchanger and in an isentropic expansion turbine. The gas cycle efficiency is a function of the compressor pressure ratio and increases with increasing pressure ratio.

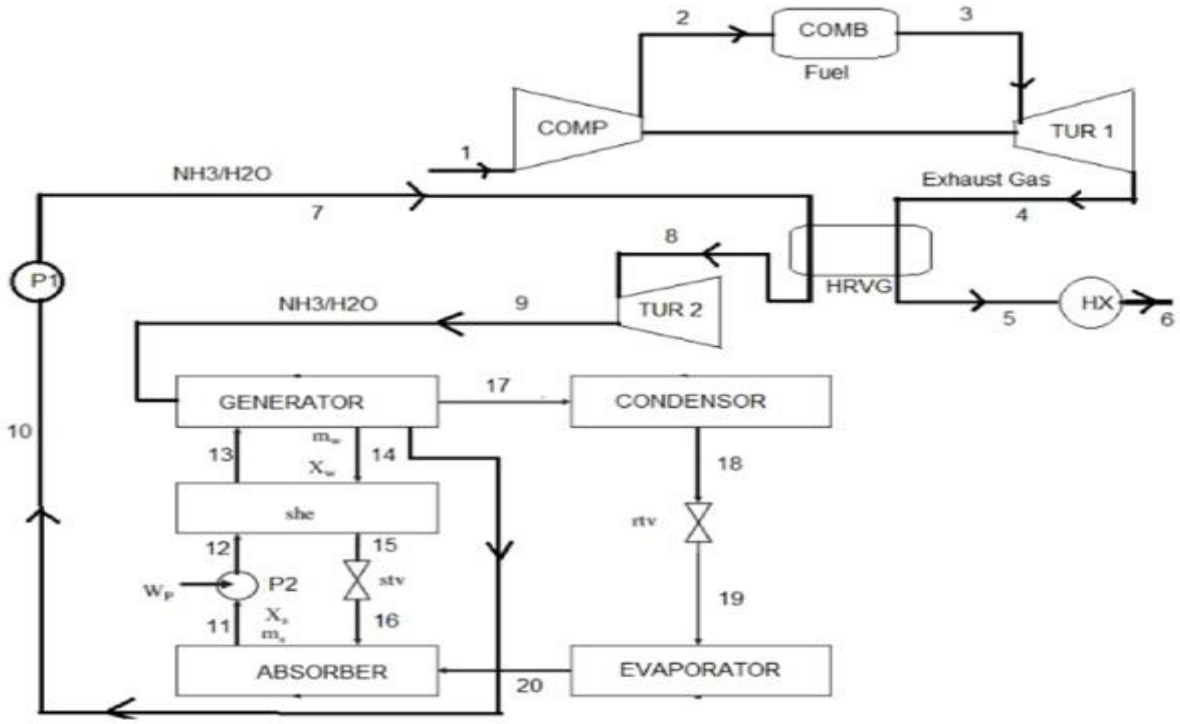

Fig. 1. The schematic of the cogeneration system is investigated

One of the most important features of the gas cycle is the high work of the compressor compared to the work of the turbine so the compressor needs 40 to 80% of the turbine power. To improve the gas cycle efficiency, methods such as increasing the turbine inlet temperature, increasing the efficiency of thermodynamic components, and using equipment such as recovery and intermediate cooling are used. The cycle of a real gas turbine is different from the ideal cycle due to the irreversibility of the turbine and compressor and the pressure drop across the flow and heat exchanger passages. In the real world, irreversibility reduces turbine performance and increases compressor performance. Turbine production work is less than ideal and compressor work required is more than ideal. The absorption refrigeration cycle is economically significant. In this system, the refrigerant is absorbed by a transfer interface. The most widely used adsorption refrigeration system is the water-ammonia system, which is refrigerant ammonia and transfer water. In the water-lithium bromide and water-lithium chloride absorption refrigeration cycle, water is used as a refrigerant and they are used when the minimum temperature is higher than the freezing point of water. Absorption refrigeration system has advantages such as the availability of a cheap source and suitable for generating heat. Disadvantages of the absorption refrigeration system are more difficult than steam compression refrigeration, such as being more expensive, requiring more space, lower efficiency, the need for larger cooling towers to dissipate excess heat and maintenance service. A salient feature of the absorption system is that it requires a small amount of work because the pumping process is done only for the liquid.

3. System Evaluation

3.1. Gas Turbine Cycle Energy Analysis

In the gas cycle, we examine the governing relationships in calculating compressor and turbine operation, combustion chamber heat, and other components. The heat exchanged in the steam heat exchanger generator is obtained from the following equation [36]:

$$Q_{HRVG} = m_4(h_5 - h_4) \quad (1)$$

The heat exchanged in the combustion chamber is obtained from the following equation [36]:

$$Q_{comb} = m_{dot}(h_3 - h_2) \quad (2)$$

The network exchanged in the gas cycle is calculated from the following equation [36]:

$$W_{net_{gas}} = m_{dot}\left(w_{a_{turb_1}} - w_{a_{comp}}\right) \quad (3)$$

The efficiency of the gas turbine cycle is calculated by this relation [36]:

$$\eta_{total_{gas}} = \frac{W_{net_{gas}}}{Q_{comb}} \quad (4)$$

The pressure ratio in the compressor is 6.7 and the isotropic efficiency of the compressor and turbine is 0.84 and 0.87, respectively.

3.2. Gas Turbine Cycle Exergy Analysis

Exergy elimination in gas cycle components is calculated by the following equations [36]:

$$E_{dist_{comp}} = m_{dot}(h_1 - T_0 \times s_1) - m_{dot}(h_2 - T_0 \times s_2) + m_{dot}\left(w_{a_{comp}}\right) \quad (5)$$

$$E_{dist_{comb}} = m_{dot}(h_2 - T_0 \times s_2) - m_{dot}(h_3 - T_0 \times s_3) + Q_{comb}(1 - \frac{T_0}{T_H}) \quad (6)$$

$$E_{dist_{turb_1}} = m_{dot}(h_3 - T_0 \times s_3) - m_{dot}(h_4 - T_0 \times s_4) - m_{dot}(w_{a_{turb}}) \quad (7)$$

$$E_{dist_{hx}} = m_{dot}(h_5 - T_0 \times s_5) - m_{dot}(h_6 - T_0 \times s_6) \quad (8)$$

3.3. Water Cycle Energy Analysis – Ammonia

In the water-ammonia cycle, the operation of the turbine and the pump are calculated by the following equations [37]:

$$W_{p\_1} = (m_{10} \times v_{10}(p_7 - p_{10}))/\ \eta_{\text{pump\_1}} \quad (9)$$

$$W_{turb_{2_s}} = m_8(h_8 - h_{9_s}) \quad (10)$$

$$W_{turb_{2_a}} = m_8(h_8 - h_9) \quad (11)$$

The isotropic efficiency of the turbine is obtained from the following equation [37]:

$$\eta_{turb_2} = \left(\frac{h_9 - h_8}{(h_{9_s} - h_8)}\right) \quad (12)$$

The network of the water-ammonia cycle is obtained from the following relation [37]:

$$W_{net_{water-ammonia}} = m_{dot}\left(w_{a_{turb_2}} - w_{pump_1}\right) \quad (13)$$

3.4. Exergy Analysis of Water Cycle Energy – Ammonia

The elimination of exergy in a water-ammonia turbine is obtained from the following equation [37]:

$$E_{dist_{turb_2}} = m_{dot}(h_8 - T_0 \times s_8) - m_{dot}(h_9 - T_0 \times s_9) - m_{dot}\left(w_{a_{turb_2}}\right) \quad (14)$$

The isotropic efficiencies of turbine two and pump one are 0.88 and 0.7, respectively.

3.5. Energy Analysis of Water-Lithium Absorption Cycle

The relationships between heat calculation and component work in the water-lithium bromide absorption refrigeration cycle are as follows [38]. The Performance coefficient of the absorption refrigeration cycle is calculated from the following relation:

$$\text{Cop} = (Q_{evap}/(Q_{gen} + W_{pump_2})) \quad (15)$$

The work of the absorption refrigeration cycle is calculated from the following relation:

$$W_{\text{net}_{\text{jazb}}} = \text{W}_{\text{pump}_2} \quad (16)$$

3.6. Exergy Analysis of Water-Lithium Absorption Cycle

Exergy destruction of water-lithium bromide absorption refrigeration components is obtained from the following equations [38]:

$$E_{dist_{abs}} = m_{20}(h_{20} - T_0 \times s_{20}) + m_{16}(h_{16} - T_0 \times s_{16}) - m_{11}(h_{11} - T_0 \times s_{11}) - Q_{abs}\left(1 - \frac{T_0}{T_{abs}}\right) \quad (17)$$

$$E_{dist_{gen}} = m_{13}(h_{13} - T_0 \times s_{13}) - m_{14}(h_{14} - T_0 \times s_{14}) - m_{17}(h_{17} - T_0 \times s_{17}) - Q_{gen}\left(1 - \frac{T_0}{T_{gen}}\right) \quad (18)$$

$$E_{dist_{cond}} = m_{17}(h_{17} - T_0 \times s_{17}) - m_{18}(h_{18} - T_0 \times s_{18}) - Q_{cond}\left(1 - \frac{T_0}{T_{cond}}\right) \quad (19)$$

$$E_{dist_{evap}} = m_{19}(h_{19} - T_0 \times s_{19}) - m_{20}(h_{20} - T_0 \times s_{20}) - Q_{evap}\left(1 - \frac{T_0}{T_{evap}}\right) \quad (20)$$

$$E_{dist_{SHE}} = m_{12}(h_{12} - T_0 \times s_{12}) + m_{14}(h_{14} - T_0 \times s_{14}) - m_{13}(h_{13} - T_0 \times s_{13}) - m_{15}(h_{15} - T_0 \times s_{15}) \quad (21)$$

$$E_{dist\_stv} = m_{15}T_{10}(s_{16} - s_{15}) \quad (22)$$

$$E_{dist\_rtv} = m_{18}T_{10}(s_{19} - s_{18}) \quad (23)$$

3.7. Energy Analysis of the Whole System

The net work of the whole system is calculated from the following equation [39]:

$$W_{\text{net}_{\text{total}}} = W_{net_{gas}} + W_{net_{water-ammonia}} + W_{\text{net}_{\text{jazb}}} \quad (24)$$

The efficiency of the whole system is calculated from the following equation [39]:

$$\eta_{cchp} = \frac{(Q_{heating} + Q_{cooling} + W_{net_{total}})}{m_{fuel} \times LHV_{fuel}} \quad (25)$$

3.8. Exergy Analysis of the Whole System

Exergy efficiency is obtained from the following equation [39]:

$$\eta ex = \frac{W + E_c + E_H}{m_{fuel} \cdot \varepsilon_{fuel}} \quad (26)$$

The cooling exergy output is obtained from the following equation [39]:

$$E_c = m_{ref}\left[\left(\left(h_{EVA,in} - h_{EVA,out}\right)\right) - T_0\left(S_{EVA,in} - S_{EVA,out}\right)\right] \quad (27)$$

The output of the heating exergy is obtained from the following equation [39]:

$$E_{\text{H}} = \text{Q}_{\text{H}}\left(1 - \frac{\text{T}_0}{\text{T}_{\text{H}}}\right) \quad (28)$$

The chemical exergy of the fuel is obtained from the following equation [39]:

$$\varepsilon_{fuel} = LHV(1.033 + 0.0169\frac{b}{a} - \frac{0.0698}{a}) \quad (29)$$

Using electricity purchased from the grid, cooling produced by a compression chiller and heating from a natural boiler, fuel consumption is shown by the following relation [39]:

$$F_{sp} = \frac{W}{\eta_g} + \frac{Q_c/cop_e}{\eta_g} + \frac{Q_H}{\eta_b} \quad (30)$$

In this regard, the efficiency of the generator is equal to 0.33 and the efficiency of the boiler is 0.8.

4. Economic Evaluation

The total cost function is defined as the sum of the operating cost rate, which is related to the fuel cost and the cost rate, which is a symbol of investment and maintenance costs. Therefore, the total cost function represents the total cost

rate in dollars per unit of time, which is represented by this relation [40]:

$$C_T = C_{env} + C_{fuel} + \sum C_{CIM} \quad (31)$$

The first is the cost of carbon dioxide, the second is the cost of fuel, and the third is the rate of investment and maintenance. Where c is the point cost of fuel per unit of energy, m is the mass flow rate of the fuel. To convert capital investment to cost rate and calculate investment rate and capital maintenance, the following equation is used for different components of the system [40]:

$$C_{CIM} = CRF \times \frac{\varphi_r}{(N \times 3600)} \times PEC_k \quad (32)$$

where PEC is a function of purchase cost, expressed in terms of system thermodynamic parameters. CRF is the economic parameter that depends on the interest rate and the life of the estimated equipment. Which is obtained by the following relation [40]:

$$CRF = \frac{i(1+i)^n}{(1+i)^n - 1} \quad (33)$$

The cost functions of the system components are calculated as follows [40-43]:

$$PEC_{comp} = \left(\frac{39.5 \times m_2}{0.9 - eta_{comp}}\right)\left(\frac{P_2}{P_1}\right)\ln\left(\frac{P_2}{P_1}\right) \quad (34)$$

$$PEC_{comb} = \left(\frac{46.08 \times m_2}{0.995 - \frac{P_3}{P_2}}\right) \times (1 + \exp(0.018 \times T_3 - 26.4)) \quad (35)$$

$$PEC_{gas\ turbine} = \left(\frac{479.34 \times m_3}{0.92 - eta_{gas\ turbine}}\right) ln\left(\frac{P_3}{P_4}\right)(1 + \exp(0.036 \times T_3 - 54.4)) \quad (36)$$

$$PEC_{HRVG} = \left(\frac{576.1}{397}\right) C_{0_{HRVG}} \times \left(B_{1,HRVG} + B_{2,HRVG} \times F_{M_{HRVG}} \times F_{P_{HRVG}}\right) \quad (37)$$

$$PEC_{pump\_2} = 1120 \times {W_{pump_2}}^{0.8} \quad (38)$$

$$PEC_{evap} = 1397 \times {A_{evap}}^{0.89} \quad (39)$$

$$PEC_{cond} = 1397 \times {A_{cond}}^{0.89} \quad (40)$$

$$PEC_{she} = 383.5 \times {A_{she}}^{0.65} \quad (41)$$

$$PEC_{abs} = 16500 \times (0.01 \times A_{abs})^{0.6} \quad (42)$$

$$F_{p_{HRVG}} = \exp\left(Y_{-1_{HRVG}} + Y_{-2_{HRVG}} \times 4.11 + Y_{-3_{HRVG}} \times (4.11)^2\right) \quad (43)$$

$$c_{0\_turb\_2} = \exp\left(k_{\_1\_turb\_2} + k_{\_2\_turb\_2} + k_{\_3\_turb\_2}\right) \quad (44)$$

$$c_{0\_HRVG} = \exp\left(k_{-1_{HRVG}} + k_{-2_{HRVH}} \times 1.26 + k_{\_3\_HRVG} \times (1.26)^2\right) \quad (45)$$

The fixed values of economic analysis are shown in Table 1.

Table. 1. Fixed values of economic analysis [23]

Parameter	Value
$k_{\_1\_turb\_2}$	2.705
$k_{\_2\_turb\_2}$	1.44
$k_{\_3\_turb\_2}$	-0.1776
$k_{\_1\_HRVG}$	4.325
$k_{\_2\_HRVG}$	-0.303
$k_{\_3\_HRVG}$	0.1634
$B_{\_1\_pump}$	1.89
$B_{\_2\_pump}$	1.35
$B_{\_1\_HRVG}$	1.63
$B_{\_2\_HRVG}$	1.66
$Y_{\_1\_HRVG}$	0.03881
$Y_{\_2\_HRVG}$	0.11272
$Y_{\_3\_HRVG}$	0.08183
F_{M_pump}	2.2
C_{fuel}	8.58
F_{p_pump}	1.8
F_{M_HRVG}	1
$F_{\_BM\_turb}$	3.5

The preliminary data used in the research are shown in Table 2:

Table. 2. Basic data in thermodynamic calculation

Parameter	Value
First pump efficiency (%)	70
Combustion chamber efficiency (%)	99
First turbine efficiency (%)	87
compression ratio	6.7
Heat exchanger efficiency (%)	70
Compressor efficiency (%)	84
Second turbine efficiency (%)	88
Interest rate (%)	14
Performance period (year)	15
Annual operating hours (hour)	7300
Maintenance coefficient	1.06

Corresponding to Figure 2, the temperature-entropy (T-s) diagram of the proposed system is presented. In this research, we have tried to calculate the state of that point and its other properties including, enthalpy, entropy and exergy, by using EES software and having two independent properties of each point. During this study, it is assumed that the quiescent temperature is 25 ° C and the quiescent pressure is 1.013 atmospheres. Heat loss in system components is neglected, and the performance of system components is assumed to be stable. The simulation is based on mass and energy conservation, and the default convergence error is 0.01%.

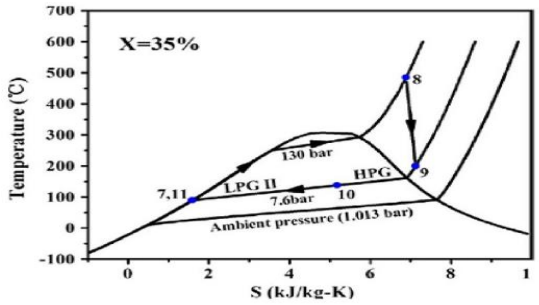

Fig. 2. T-S diagram of the proposed system

5. Validation

In this research, validation was done using the work of Arora et al. In the operating conditions, it is assumed that the quiescent temperature is 25 ° C, the quiescent pressure is 101 kPa, the generator temperature is 87.8 ° C, the evaporator temperature is 7.2 ° C, the condenser and absorber temperature is 37.8 ° C. C, low pressure is 1.0161 kPa and high pressure is 6.558 kPa and validation has been done and it is shown in Table 3 which shows good results. The thermodynamic properties of different parts of the system are shown in Table 4.

Table 3. Validation of the proposed system with the evaluation of Arora et al. [38]

Parameter	Obtained results	Reference results
Absorbent heat (kW)	2943	2945.26
Condenser heat (kW)	2506	2505.91
Evaporator heat (kW)	2355	2355.4
Coefficient of performance	0.79	0.7609
Absorptive exergy destruction (kW)	70.16	70.478
Condenser exergy destruction (kW)	6.606	6. 066
Evaporator exergy destruction (kW)	86.28	86.275

Table. 4. Energy analysis results

Point	T(C)	P(kPa)	h(kJ/kg)	S(kJ/kgK)	e (kJ/kg)	$\dot{m}\left(\frac{kg}{s}\right)$
1	25	101.3	298.6	5.695	0.2538	7.832
2	280.4	678.7	558.8	5.778	235.8	7.832
3	1155	651.6	1549	6.85	906.2	8.7
4	637	97.25	944.6	6.872	295.4	8.7
5	170	101.3	445.1	6.096	27.49	8.7
6	90	101.3	364	5.894	6.464	8.7
7	93.19	13000	205.6	1.152	44.38	1.521
8	500	13000	3064	6.458	1320	1.521
9	206.3	970	2460	6.636	633.4	1.521
10	90	970	184.6	1.135	28.58	1.521
11	37.8	1.016	91.46	0.2287	1723	10.54
12	37.8	6.558	91.46	0.2287	1723	10.54
13	72.84	6.558	163.2	0.4472	1730	10.54
14	87.8	6.558	221.2	0.4791	1778	9.374
15	52.8	6.558	156.2	0.2895	1770	9.374
16	52.8	1.016	156.2	0.2895	1770	9.374
17	87.8	6.558	2664	8.58	110.8	1.166
18	37.8	6.558	158.3	0.5428	1.023	1.166
19	7.2	1.016	158.3	0.5661	5.913	1.166
20	7.2	1.016	2514	8.968	155.5	1.166

As shown in Table 5, the greatest destruction of exergy takes place in the combustion chamber, which is caused by the large temperature difference in it.

Table. 5. Exergy destruction of components

Parameter	Value
Condenser (kW)	7.701
Expansion valve (kW)	8.085
Combustion chamber (kW)	1628
Steam heat exchanger (kW)	10.32
Compressor (kW)	193.4
Evaporator (kW)	100.6
Generator (kW)	58.18
First Turbine (kW)	57.28
Absorbent (kW)	81.79
Heat exchanger (kW)	182.9
Second turbine (kW)	80.8

The results of the thermodynamic analysis are shown in supplementary Table 6.

Table. 6. Energy efficiency and exergy system results

Parameter	Value
Energy efficiency (%)	21.29
Exergy efficiency (%)	20.68
Fuel consumption coefficient	25890
Absorption refrigeration system performance coefficient (%)	79.24

According to Table 7, the results of the economic analysis of the system show that the steam heat exchanger generator has the highest exergy destruction.

Table. 7. Costs of system components cost

Parameter	Value
Absorber ($ / s)	40816
Turbine One ($ / s)	166482
Double turbine ($ / s)	1311506
Condenser ($ / s)	160830
Heat exchanger generator ($ /s)	4174477
Combustion chamber ($ / s)	10349
Pump one ($ / s)	17851
Compressor ($ / s)	65713
Double pump ($ / s)	4470
Evaporator ($ / s)	323004
Steam heat exchanger ($ / s)	7696
Generator ($ / s)	19484
Fuel ($ / s)	85.88
Carbon Dioxide ($ / s)	87
Total system ($ / s)	93.56

6. Impact of Density Ratio Changes on System Performance

As shown in Figure 3, fuel consumption decreases with increasing pressure ratio. This is due to the increase in air temperature that enters the combustion chamber. That is, when the temperature rises, less fuel is used to meet the needs of heat balance. In addition, with an increasing pressure ratio, cold production increases. In addition, power generation increases to a maximum and then decreases.

By increasing the compression ratio in the compressor, according to Figure 4, the energy efficiency and exergy decrease. Increasing the performance of the air compressor at a lower pressure ratio is less than a higher pressure ratio. Thus, net power generation first increases and then decreases at a higher pressure ratio. By increasing the pressure ratio, the exergy degradation in the combustion chamber is significantly reduced. This is because increasing the pressure ratio means less exergy difference between compressed air and combustion products. Higher pressure ratios increase the amount of combustion energy in the combustion products and reduce the amount of exhaust gas in the turbine, which results in more power dissipation in the turbine.

Finally, increasing the pressure ratio leads to an increase in the velocity of the steam flow that enters the absorption chiller, which in turn increases the exergy degradation in the chiller. As the density ratio increases, cold production increases, heat production and fuel consumption decrease, and net power first increases at lower density ratios and decreases at higher values.

The changes in net work relative to the pressure ratio are shown in Figure 7. As the ratio of net working pressure and the cost function increases, system cycles increase.

Changes in total cost and total exergy destruction and exergy destruction of gas, water-ammonia and absorption refrigeration cycles relative to the pressure ratio are shown in Figures 5 and 6.

As the pressure ratio increases, the total cost increases and the total exergy destruction and exergy destruction of the system cycles decreases. In addition, the exergy degradation in the air compressor increases with increasing pressure ratio. This is because more heat is generated in the air compressor with a higher pressure ratio.

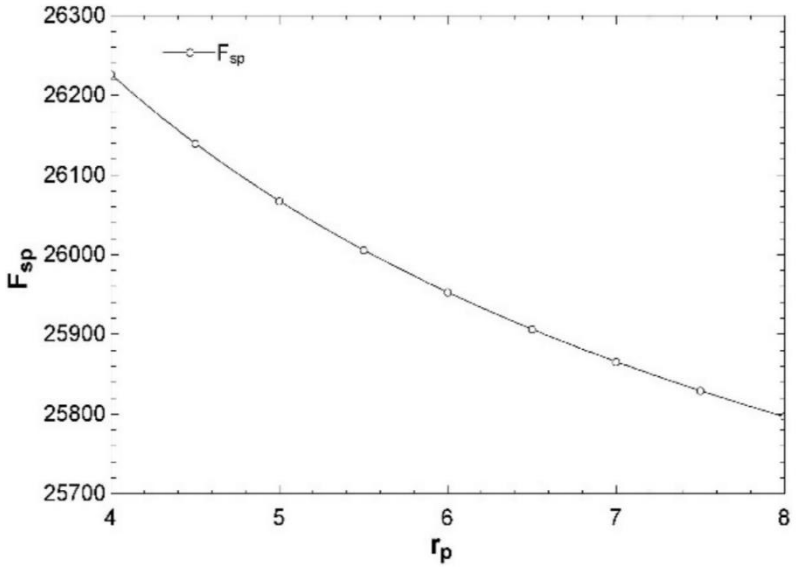

Fig. 3. The effect of density ratio on fuel consumption storage coefficient

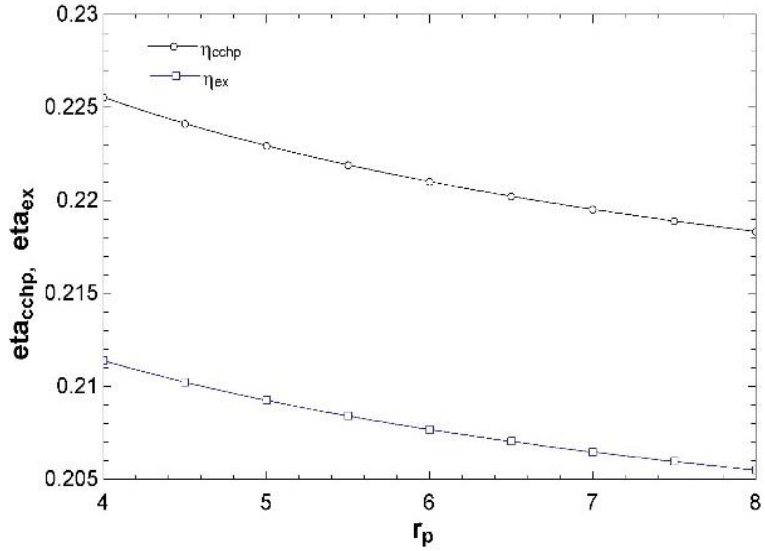

Fig. 4. The effect of density ratio on energy efficiency and exergy

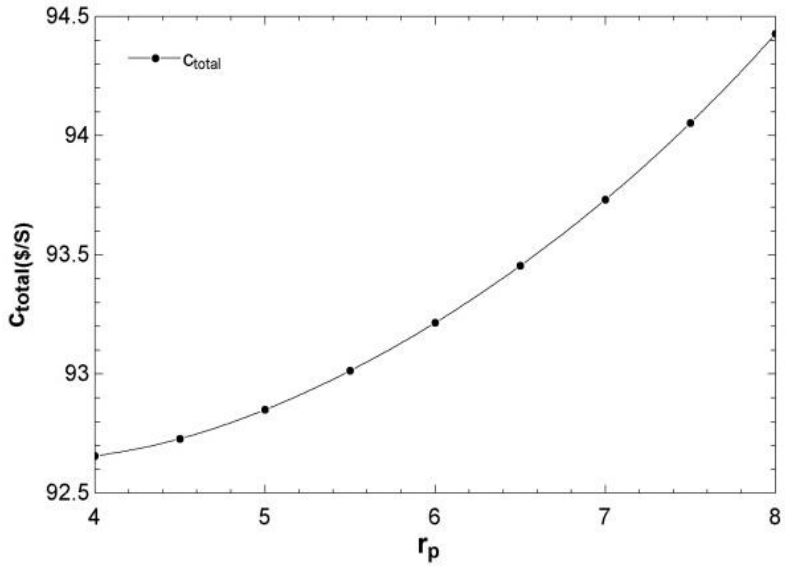

Fig. 5. Impact of density ratio on total cost

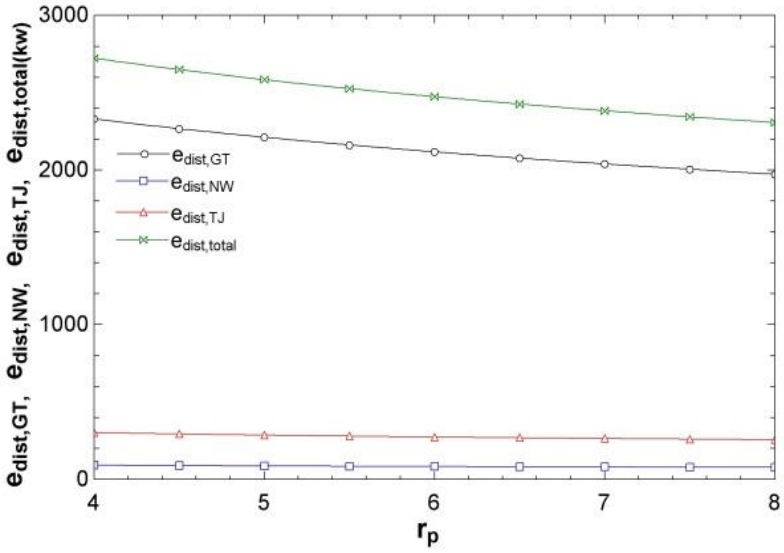

Fig. 6. The effect of density ratio on the exergy destruction of system cycles

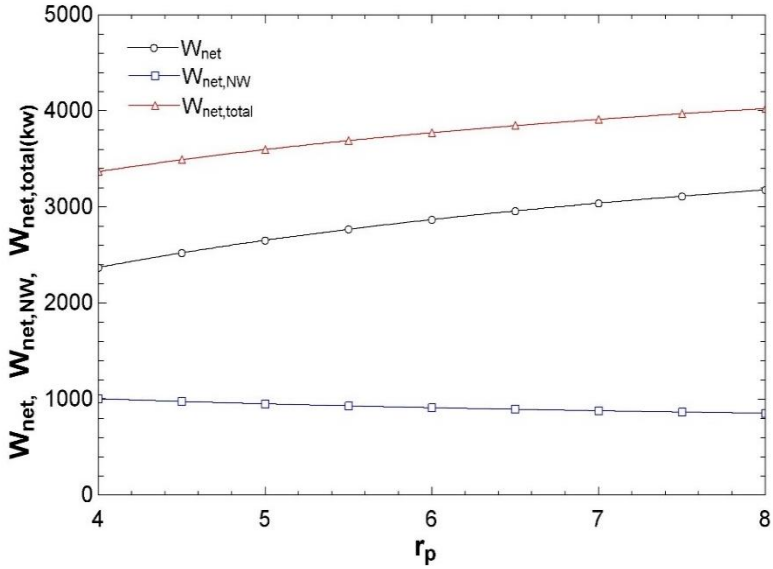

Fig. 7. The effect of density ratio on the work of system cycles

7. The Effect of Changes in the Molar Coefficient of Air on System Performance

Graphs of changes in fuel consumption coefficient and efficiency of the first and second laws of thermodynamics relative to the molar coefficient of inlet air in the combustion chamber are shown in Figures 8 and 9. By increasing the molar coefficient of the intake air, the efficiency of the energy law and exergy of the system decreases by 9%, the performance of the system decreases, and the fuel storage coefficient of the consumed fuel decreases by 47%. Increasing the molar coefficient of the inlet air to the gas turbine causes the system to move away from complete combustion conditions and the ideal state.

The changes in exergy destruction and total net work, gas and water-ammonia cycles and absorption refrigeration relative to the molar coefficient of the combustion chamber inlet air are shown in Figures 10 and 11. Increasing the molar coefficient of air reduces the efficiency of the system and increases the elimination of exergy in the system, thus reducing the net work and power output of the system. Compression ratio, ambient temperature, air to fuel ratio as well as isentropic efficiency strongly affect the thermal efficiency of gas turbine power plant. Changing the thermal efficiency at higher compression ratios, turbine inlet temperatures and ambient temperatures is very important.

The graph of system cost changes relative to the molar ratio of the inlet air to the combustion chamber is shown in Figure 12. By increasing the molar coefficient of air, the cycle cost of the gas system decreases and remains constant after the molar coefficient of 2.3 and does not change

much. With increasing ambient temperature as well as air to fuel ratio, thermal efficiency and power output decrease linearly. As the ambient temperature and the ratio of air to fuel increase, the amount of fuel consumption and the amount of heat increase linearly. Maximum efficiency, power and specific fuel consumption occur at higher compression ratios with lower ambient temperatures.

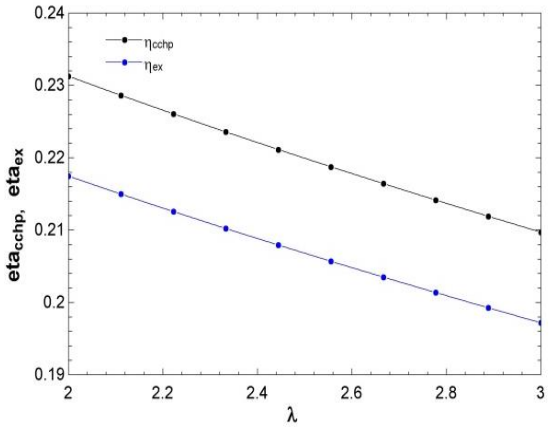

Fig. 8. Effect of molar coefficient of air entering the combustion chamber on energy efficiency and exergy

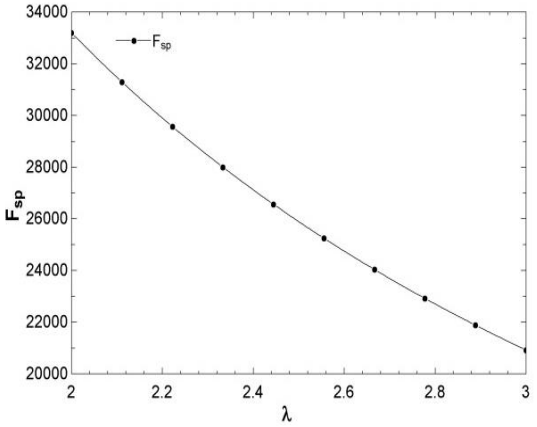

Fig. 9. The effect of molar coefficient of air entering the combustion chamber on fuel consumption storage coefficient

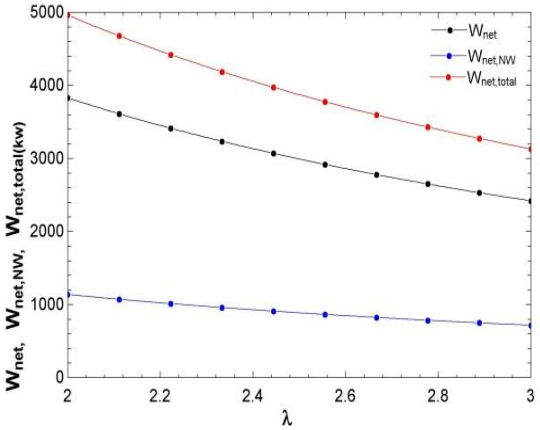

Fig. 10. The effect of the molar coefficient of the air entering the combustion chamber on the operation of the system cycles

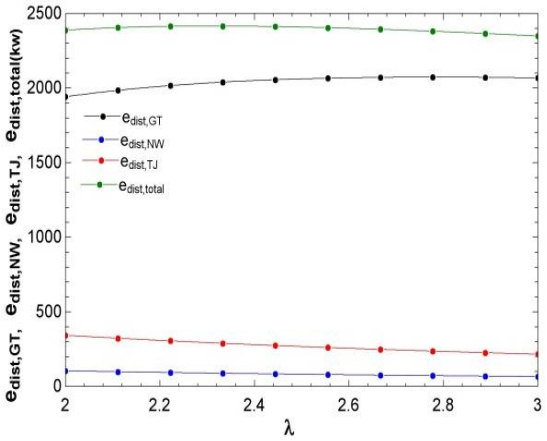

Fig. 11. The effect of the molar coefficient of the air entering the combustion chamber on the exergy destruction of the system cycles

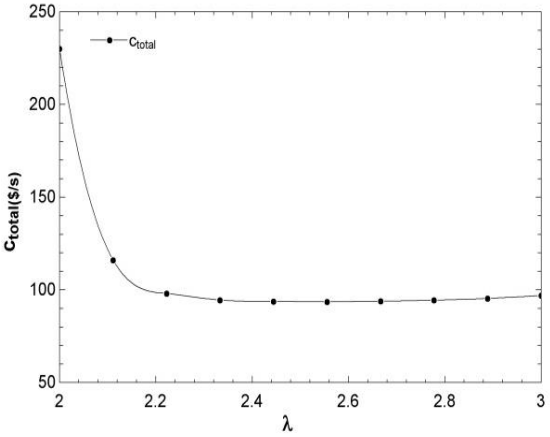

Fig. 12. The effect of the molar coefficient of the air entering the combustion chamber on the total cost

8. Conclusions

In this study, an effective step was taken to optimize energy consumption and reduce environmental pollution. This research has proposed and analyzed a new combined heating and power system consisting of a gas turbine, a combined cooling and power subsystem and a hot water heat exchanger. - Ammonia and water absorption refrigeration - Ammonia is formed. The waste heat in the gas turbine is used to create cooling by the evaporator in the absorption refrigeration cycle. By using this system in the place of energy consumption, the costs of transferring the generated power from the production network to the place of consumption can be reduced, and the consumption of primary energy can be reduced. The electricity generated by the ammonia water turbine can be used in part or in part to run a pressure chiller to generate cooling energy. Comprehensive thermodynamic modeling for a third-generation system based on a single-effect absorption chiller has been performed. Exergy analysis showed that the combustion chamber and heat recovery boiler

have the highest exergy destruction compared to other components of the system. This is mainly due to the large temperature difference for heat transfer in both mentioned components and the combustion reaction in the combustion chamber. System performance is significantly affected by changes in compressor pressure ratio, inlet temperature to gas turbine and isotropic efficiency of high temperature generator. Energy dissipation in the absorption chiller is less than that of other components. As the compressor pressure ratio increases, the exergy efficiency decreases and the carbon dioxide emission increases. The efficiency of the system increases with increasing isotropic efficiency of the gas turbine. The energy efficiency of a gas turbine increases with increasing turbine inlet temperature. The energy efficiency of the system is 21%, and the exergy efficiency of the system is 20%. The use of simultaneous generation systems of power, heat and cold is an efficient step to increase the efficiency and efficiency of electricity generation and in terms of reducing energy consumption. By applying modifications to the combustion chamber, such as increasing the inlet temperature to the chamber, and applying complete combustion conditions and reducing excess air, maximum exergy destruction can be reduced, and carbon dioxide emissions and emissions to the environment can be reduced and an effective step to reduce environmental pollution. Environmentally, it preserves the ozone layer and prevents temperature inversion and acid rain. As the pressure ratio and the total cost increase, the fuel consumption storage coefficient and the total exergy destruction decrease. As the turbine inlet mass flow rate increases, the fuel consumption storage coefficient, the total cost, the total exergy elimination and the energy and exergy efficiency increase. By increasing the molar ratio of combustion inlet air, the energy and exergy efficiency, the total cost and the fuel consumption storage coefficient decrease.

Funding Statement

This research did not receive any specific grant from funding agencies in the public, commercial, or not-for-profit sectors.

Conflicts of Interest

The author declares that there is no conflict of interest regarding the publication of this article.

Availability of data and material

The data will be made available on request.

References

[1] Balal, A., Sheikhzadeh, G. A., & Fattahi, A., 2024. Experimental evaluation of the hybrid-bifacial cooling of a PV panel in an arid weather using channel heat exchanger and impingement flow nozzles. Journal of Heat and Mass Transfer Research, 11(2), pp. 195-210.

[2] Li, X., Xu, B., Tian, H. and Shu, G., 2021. Towards a novel holistic design of organic Rankine cycle (ORC) systems operating under heat source fluctuations and intermittency. Renewable and Sustainable Energy Reviews, 147, p.111207.

[3] White, M.T., Bianchi, G., Chai, L., Tassou, S.A. and Sayma, A.I., 2021. Review of supercritical CO2 technologies and systems for power generation. Applied Thermal Engineering, 185, p.116447.

[4] Karami, M., & Nasiri Gahraz, S. S., 2021. Transient Simulation and Life Cycle Cost Analysis of a Solar Polygeneration System using Photovoltaic-Thermal Collectors and Hybrid Desalination Unit. Journal of Heat and Mass Transfer Research, 8(2), pp. 243-256.

[5] Bahoosh, R., Nazeri, A., Changizian, M., & Moravej, M., 2022. Fabrication of Solar Desalination System and Experimental Investigation of its Performance, Located in Ahvaz City. Journal of Heat and Mass Transfer Research, 9(2), pp. 255-268.

[6] Bahoosh, R., Sedeh Ghahfarokhi, M. and Saffarian, M., 2018. Energy and exergy analysis of a diesel engine running with biodiesel fuel. Journal of Heat and Mass Transfer Research, 5(2), pp.95-104.

[7] Tang, J., Zhang, Q., Zhang, Z., Li, Q., Wu, C. and Wang, X., 2022. Development and performance assessment of a novel combined power system integrating a supercritical carbon dioxide Brayton cycle with an absorption heat transformer. Energy Conversion and Management, 251, p.114992.

[8] Wang, S., Zhang, L., Liu, C., Liu, Z., Lan, S., Li, Q. and Wang, X., 2021. Techno-economic-environmental evaluation of a combined cooling heating and power system for gas turbine waste heat recovery. Energy, 231, p.120956.

[9] Jiang, R., Qin, F.G., Yin, H., Yang, M. and Xu, Y., 2017. Thermo-economic assessment and application of CCHP system with

dehumidification and hybrid refrigeration. Applied Thermal Engineering, 125, pp. 928-936.

[10] Zhang, F., Liao, G., Jiaqiang, E., Chen, J. and Leng, E., 2021. Comparative study on the thermodynamic and economic performance of novel absorption power cycles driven by the waste heat from a supercritical CO2 cycle. Energy Conversion and Management, 228, p.113671.

[11] Fan, G., Li, H., Du, Y., Zheng, S., Chen, K. and Dai, Y., 2020. Preliminary conceptual design and thermo-economic analysis of a combined cooling, heating and power system based on supercritical carbon dioxide cycle. Energy, 203, p.117842.

[12] Yuan, J., Wu, C., Xu, X. and Liu, C., 2021. Proposal and thermoeconomic analysis of a novel combined cooling and power system using carbon dioxide as the working fluid. Energy conversion and management, 227, p.113566.

[13] Wu, C., Xu, X., Li, Q., Li, J., Wang, S. and Liu, C., 2020. Proposal and assessment of a combined cooling and power system based on the regenerative supercritical carbon dioxide Brayton cycle integrated with an absorption refrigeration cycle for engine waste heat recovery. Energy conversion and management, 207, p.112527.

[14] Martín-Hernández, E., Guerras, L.S. and Martín, M., 2020. Optimal technology selection for the biogas upgrading to biomethane. Journal of cleaner production, 267, p.122032.

[15] Mehrpooya, M., Ghorbani, B. and Manizadeh, A., 2020. Cryogenic biogas upgrading process using solar energy (process integration, development, and energy analysis). Energy, 203, p.117834.

[16] Ghorbani, B., Ebrahimi, A. and Ziabasharhagh, M., 2021. Thermodynamic and economic evaluation of biomethane and carbon dioxide liquefaction process in a hybridized system of biogas upgrading process and mixed fluid cascade liquefaction cycle. Process Safety and Environmental Protection, 151, pp.222-243.

[17] Hosseini, S.E., 2020. Design and analysis of renewable hydrogen production from biogas by integrating a gas turbine system and a solid oxide steam electrolyzer. Energy conversion and management, 211, p.112760.

[18] Ebrahimi, A., Ghorbani, B. and Ziabasharhagh, M., 2022. Exergy and economic analyses of an innovative integrated system for cogeneration of treated biogas and liquid carbon dioxide using absorption–compression refrigeration system and ORC/Kalina power cycles through geothermal energy. Process Safety and Environmental Protection, 158, pp.257-281.

[19] Jing, Y.Y., Bai, H. and Wang, J.J., 2012. A fuzzy multi-criteria decision-making model for CCHP systems driven by different energy sources. Energy Policy, 42, pp.286-296.

[20] Wang, J., Dai, Y., Gao, L. and Ma, S., 2009. A new combined cooling, heating and power system driven by solar energy. Renewable Energy, 34(12), pp.2780-2788.

[21] Gu, Q., Ren, H., Gao, W. and Ren, J., 2012. Integrated assessment of combined cooling heating and power systems under different design and management options for residential buildings in shanghai. Energy and Buildings, 51, pp.143-152.

[22] Yan, B., Xue, S., Li, Y., Duan, J. and Zeng, M., 2016. Gas-fired combined cooling, heating and power (CCHP) in Beijing: A techno-economic analysis. Renewable and Sustainable Energy Reviews, 63, pp.118-131.

[23] Li, M., Qin, C., Feng, Y., Zhou, M., Mu, H., Li, N. and Ma, Q., 2017. Optimal design and analysis of CCHP system for a hotel application. Energy Procedia, 142, pp.2329-2334.

[24] Wang, L., Lu, J., Wang, W. and Ding, J., 2017. Feasibility analysis of CCHP system with thermal energy storage driven by micro turbine. Energy Procedia, 105, pp.2396-2402.

[25] Okamoto, S., 2011. Saving energy in a hospital utilizing CCHP technology. International Journal of Energy and Environmental Engineering, 2(2), pp.45-55.

[26] Bruno, J.C., Valero, A. and Coronas, A., 2005. Performance analysis of combined microgas turbines and gas fired water/LiBr absorption chillers with post-combustion. Applied Thermal Engineering, 25(1), pp.87-99.

[27] Kong, X.Q., Wang, R.Z. and Huang, X.H., 2004. Energy efficiency and economic feasibility of CCHP driven by stirling engine. Energy

Conversion and Management, 45(9-10), pp.1433-1442.

[28] Ghaebi, H., Amidpour, M., Karimkashi, S. and Rezayan, O., 2011. Energy, exergy and thermoeconomic analysis of a combined cooling, heating and power (CCHP) system with gas turbine prime mover. International Journal of Energy Research, 35(8), pp.697-709.

[29] Fan, J., Hong, H., Zhu, L., Wang, Z. and Jin, H., 2017. Thermodynamic evaluation of chemical looping combustion for combined cooling heating and power production driven by coal. Energy conversion and management, 135, pp. 200-211.

[30] Tamm, G. and Goswami, D.Y., 2003. Novel combined power and cooling thermodynamic cycle for low temperature heat sources, part II: experimental investigation. J. Sol. Energy Eng., 125(2), pp. 223-229.

[31] Han, W., Sun, L., Zheng, D., Jin, H., Ma, S. and Jing, X., 2013. New hybrid absorption–compression refrigeration system based on cascade use of mid-temperature waste heat. Applied energy, 106, pp. 383-390.

[32] Chua, K.J., Yang, W.M., Er, S.S. and Ho, C.A., 2014. Sustainable energy systems for a remote island community. Applied Energy, 113, pp.1752-1763.

[33] Calise, F., Cipollina, A., d'Accadia, M.D. and Piacentino, A., 2014. A novel renewable polygeneration system for a small Mediterranean volcanic island for the combined production of energy and water: Dynamic simulation and economic assessment. Applied energy, 135, pp. 675-693.

[34] Karellas, S. and Braimakis, K., 2016. Energy–exergy analysis and economic investigation of a cogeneration and trigeneration ORC–VCC hybrid system utilizing biomass fuel and solar power. Energy conversion and management, 107, pp. 103-113.

[35] Valipour, M. S., Biglari, M., & Assareh, E. 2016. Thermal-Economic Optimization of Shell and Tube Heat Exchanger by using a new Multi-Objective optimization method. Journal of Heat and Mass Transfer Research, 3(1), pp. 67-76.

[36] Haseli, Y., Dincer, I. and Naterer, G.F., 2008. Thermodynamic analysis of a combined gas turbine power system with a solid oxide fuel cell through exergy. Thermochimica Acta, 480(1-2), pp. 1-9.

[37] Xu, X.X., Liu, C., Fu, X., Gao, H. and Li, Y., 2015. Energy and exergy analyses of a modified combined cooling, heating, and power system using supercritical CO2. Energy, 86, pp. 414-422.

[38] Arora, A. and Kaushik, S.C., 2009. Theoretical analysis of LiBr/H2O absorption refrigeration systems. International Journal of Energy Research, 33(15), pp. 1321-1340.

[39] Ghaebi, H., Amidpour, M., Karimkashi, S. and Rezayan, O., 2011. Energy, exergy and thermoeconomic analysis of a combined cooling, heating and power (CCHP) system with gas turbine prime mover. International Journal of Energy Research, 35(8), pp. 697-709.

[40] King, C.F., 1999. Analysis, Synthesis, and Design of Chemical Processes. Richard Turton, Richard Bailie, Wallace Whiting, Joseph Shaeiwitz Prentice Hall, 1998.

[41] Taheri, M.H., Mosaffa, A.H. and Farshi, L.G., 2017. Energy, exergy and economic assessments of a novel integrated biomass based multigeneration energy system with hydrogen production and LNG regasification cycle. Energy, 125, pp. 162-177.

[42] Mosaffa, A.H., Mokarram, N.H. and Farshi, L.G., 2017. Thermo-economic analysis of combined different ORCs geothermal power plants and LNG cold energy. Geothermics, 65, pp. 113-125.

[43] Farshi, L.G., Mahmoudi, S.S., Rosen, M.A., Yari, M. and Amidpour, M., 2013. Exergoeconomic analysis of double effect absorption refrigeration systems. Energy Conversion and Management, 65, pp. 13-25.